Dynamic modeling of local district heating grids with prosumers: A case study for Norway

Hanne Kauko[a,*], Karoline Husevåg Kvalsvik[a], Daniel Rohde[b], Natasa Nord[b], Åmund Utne[c]

[a] *SINTEF Energy Research, Kolbjørn Hejes vei 1B, Trondheim 7491, Norway*
[b] *Department of Energy and Process Engineering, Norwegian University of Science and Technology (NTNU), Kolbjørn Hejes vei 1B, Trondheim 7491, Norway*
[c] *Statkraft Varme AS, Sluppenvegen 17 B, 7005 Trondheim, Norway*

Abstract

District heating (DH) will play an important role in the future fossil-free energy systems by enabling increased utilization of waste heat and renewable heat sources to cover buildings' heat demand. A prerequisite for this is a reduction in the distribution temperature and shift towards decentralized heat production. In this study, dynamic modeling has been applied to study the technical, energetic and environmental impacts of including prosumers – customers who both consume and produce heat – in a local low-temperature DH grid. Four different scenarios were studied for a planned building area in Trondheim, Norway: high- and low-temperature scenarios with the entire heat demand being covered by a heat central, and two low-temperature scenarios including heat supply from prosumers. A data center and two food retail stores were considered as the prosumers, each with different location and individual characteristics for the heat supply, allowing to study their impact on the water flow in different parts of the grid. The results show that utilizing local surplus heat is a significant measure to reduce the heat demand and the environmental impact of the DH grid. Decentralized heat supply additionally contributes to reduced heat losses, due to overall lower distances to transport the heat.

Keywords: Low-temperature district heating, Thermal system modeling, Prosumers, Surplus heat, Energy planning

1. Introduction

District heating (DH) is an important technology in that it enables efficient and economical utilization of energy sources, that would otherwise be wasted, to cover buildings' heating demands [1]. DH will play an important role in the future fossil-free energy systems by enabling increased utilization of waste heat and renewable heat sources; however, a prerequisite for this is a reduction in the distribution temperatures and shift towards decentralized heat production [2, 3, 4]. With this, DH will allow reducing the load from the electric grid by utilizing DH for heating purposes instead of electricity wherever possible, hence promoting the utilization of electricity for other purposes where high-quality energy is needed, such as transport.

Reduced supply temperature level in DH provides a number of advantages. These include: (i) Reduction in the distribution heat losses [5, 6, 7]; (ii) Improved utilization of low-temperature waste heat sources from buildings and industry [3, 8]; and (iii) Improved efficiency and production capacity for solar thermal and higher COP for heat pumps [9]. Highlighting the new era of district heating, the concept of 4th generation district heating (4GDH) has been introduced by Lund et al. [3]. 4GDH refers to low-temperature DH systems with waste heat utilization, integration of renewable heat and an ability to be an integrated part of smart energy systems, including thermal, electric and gas grids.

Conventionally, DH systems have been based on large, centralized combustion plants or utilization of industrial waste heat sources, characterized by high capacities and temperature levels. Potential for utilization of industrial

*Corresponding author
Email address: hanne.kauko@sintef.no (Hanne Kauko)

This is the accepted version of an article published in Energy.
DOI: 10.1016/j.energy.2018.03.033

waste heat sources is enormous, in particular in central Europe [10]. Such waste heat sources are however often placed outside cities and require high heat demand densities in order to justify the investments required for the heat distribution system. In Norway, heavy industries with high availability of surplus heat are often located in remote places in the coast due to availability of large hydro power resources and easy access by ships.

Potential surplus heat suppliers present in urban environments are buildings with large chiller and refrigeration facilities, such as data centers, office buildings or food retail stores. Such buildings may have a demand for heat at low ambient temperatures and surplus heat available otherwise, and are thus referred to as heat prosumers. Urban waste heat recovery with prosumers is already practiced in for instance Stockholm under the Open District Heating Concept [11]. The impact of including prosumers in a DH grid has also been studied by the scientific community, considering the energy balance and environmental impact [8], as well as the technical challenges [12, 13]. Brange et al. [8] studied the potential of prosumers for a building area in Sweden with a high number of prosumers, including e.g. supermarkets and an indoor ice skating rink, concluding that the prosumers could potentially cover the entire heating demand of the area. Electricity would however be needed to obtain the required temperature levels, either with heat pumps or direct electric heating, and the environmental impact of the DH system with prosumers hence depends on the source of the electricity. Lennermo et al. [12] and Brand et al. [13] have reported on problems with differential pressure in the DH network, resulting from decentralized heat supply by solar collectors at a lower temperature level, and rapidly varying heat demand. This calls for proper control strategies when introducing decentralized heat suppliers in DH systems.

Due to the high investment costs related to DH systems, there is a great interest in simulation and planning software to find the most optimal solutions regarding production and distribution of heat [14]. Such tools will become increasingly important with the increased complexity of 4GDH grids including decentralized heat production by prosumers, often in combination with thermal storage and an advanced control system. There are many software tools available for simulation of DH systems; a comprehensive overview has been given in [15]. For detailed physical modeling of DH systems, the dynamic simulation program Dymola using the object-oriented modeling language Modelica has been proven to be a flexible and efficient tool [6, 14, 16, 17, 18].

In a previous study [7], a component library for modeling local DH grids was created in Dymola in order to study and compare different scenarios with various supply temperature levels for the local DH grid. For the the present study, the component library has been improved and extended to study the impact of including prosumers in a local low-temperature DH grid. Two types of prosumers were included, a data center and food retail stores, each with different, dynamic characteristics for the surplus heat delivery as well as different placement in the local DH grid. This enabled detailed investigation of the fluid flow in different parts of the grid during varying amounts of surplus heat delivery. The remaining heat demand was covered by a heat central, assumed to have the same energy mix as the DH supplier in Trondheim. The heating grid with prosumers was compared with two baseline cases, a high- and a low-temperature heating grid, in which the heat demand was entirely supplied by the heat central.

The objectives of this study are to (i) demonstrate dynamic modeling of a heating grid with prosumers; (ii) investigate the technical challenges related to inclusion of prosumers; and (iii) study the energetic and environmental benefits of surplus heat delivery.

2. Methodology

The methodology consisted of the following primary steps:

1. Collecting data for DH demand profiles for modern buildings representing different building categories, located in Trondheim (see [7]).
2. Upgrading the Dymola model for a local DH grid from the previous study [7], including new and improved components.
3. Simulating different scenarios for a local low-temperature grid with and without prosumers, and comparing the results to a reference, high-temperature scenario representing the current practice of the local DH provider.
4. Calculating the equivalent CO_2 emissions for the different simulated scenarios.

These phases are described in more detail in the following.

This is the accepted version of an article published in Energy.
DOI: 10.1016/j.energy.2018.03.033

2.1. The building stock

The investigated building area was a new neighborhood, Brøset, which is planned to be built in Trondheim, Norway. The area included several different types of buildings, such as apartment blocks, nurseries, schools, nursing homes and commercial buildings, with a total heated area of 188 000 m^2 (excluding prosumers). The DH demand of the buildings was modelled entirely from the basis of real DH use data from existing buildings, with the building type and standard matching with the buildings to be built as well as possible. Apart from a few historical buildings, the applied DH demand data were retrieved solely from new buildings. The data included the total heating demand, i.e., both space heating and DHW preparation. From this data, DHW demand profiles were extracted by analyzing the average demand for summer months (June-August), when the space heating demand is minimal. The motivation to use existing data was to be able to model the simultaneity of peaks in heat demand throughout a day and the year as realistically as possible. For more detailed description of the modelled building area, see [7].

Apartment blocks constitute the largest share (75 %) of the building mass at Brøset. In the previous work [7], the DH demand for all the apartment blocks was based on the DH demand profile of one existing building. As a result, the total DH demand profile for Brøset became unrealistically homogeneous. Hence, in the present study, three different demand profiles were used for the apartment blocks, yielding a more realistic compound profile, and an increase in the demand by 12 %. The results from [7] will be compared with the present results throughout the paper.

The total annual DH demand for the area was 12 470 MWh, out of which 5 640 MWh was for DHW heating and 6 830 MWh for space heating. The linear heat demand density was 1.82 MWh/(m · year), corresponding to a total pipeline length of 6 840 m.

2.2. Modeling approach

Dymola is a dynamic simulation software (DYnamic MOdeling LAboratory) [19], using the object-oriented modeling language Modelica. Object-oriented approach allows full re-usability, extensibility and adaptability of the created models. Furthermore, Modelica is an equation-based modeling language, meaning that it allows declaring relations among variables. Hence, the variables do not need to have explicit expressions; the Modelica code is transformed into efficient simulation code by Dymola using symbolic manipulation. An in-depth discussion of equation-based (acausal) modeling tools for energy system modeling and their advantages and disadvantages can be found in [18] and [20].

Previously, an in-house component library for modeling thermal grids has been created in Dymola. This component library is under constant development to reduce simulation time and to enable various simulation case studies. The in-house component library includes models for primary components for transport of heat and fluid, such as sensors, valves, pumps and pipes. More complicated models were built from the primary components, e.g. heat exchangers, twin-pipes surrounded by the ground, and customer substations. The modelled network included the building stock, i.e. customer substations for different types of buildings, prosumers, piping network, and a heat supply plant delivering heat at the desired temperature level and the required pressure. These components are described in more detail below, and an outline of the local DH grid model in Dymola is shown in Figure 1.

2.2.1. Number of transfer units (NTU) heat exchanger model

In an earlier version of the model [7], the heat exchanger was discretized into a number of individual cells along the length of the heat exchanger, each with a different average temperature. A high number of cells was required to obtain realistic return temperatures, increasing the computation time. For the present study, a heat exchanger model based on the NTU method was developed. In the NTU method, the heat flow in the heat exchanger is calculated from the state of the inlet streams using an analytical equation [21]:

$$Q_{flow} = \epsilon \cdot C_{min} \cdot (T_{inlet,hot} - T_{inlet,cold}), \tag{1}$$

where ϵ is the effectiveness of the heat exchanger, that is, the ratio of the actual heat transfer rate to the maximum heat transfer rate. C_{min} is the minimum heat transfer rate:

$$C_{min} = min(C_{cold}, C_{hot}) = C_p \cdot min(C_p \dot{m}_{hot}, C_p \dot{m}_{cold}), \tag{2}$$

This is the accepted version of an article published in Energy.
DOI: 10.1016/j.energy.2018.03.033

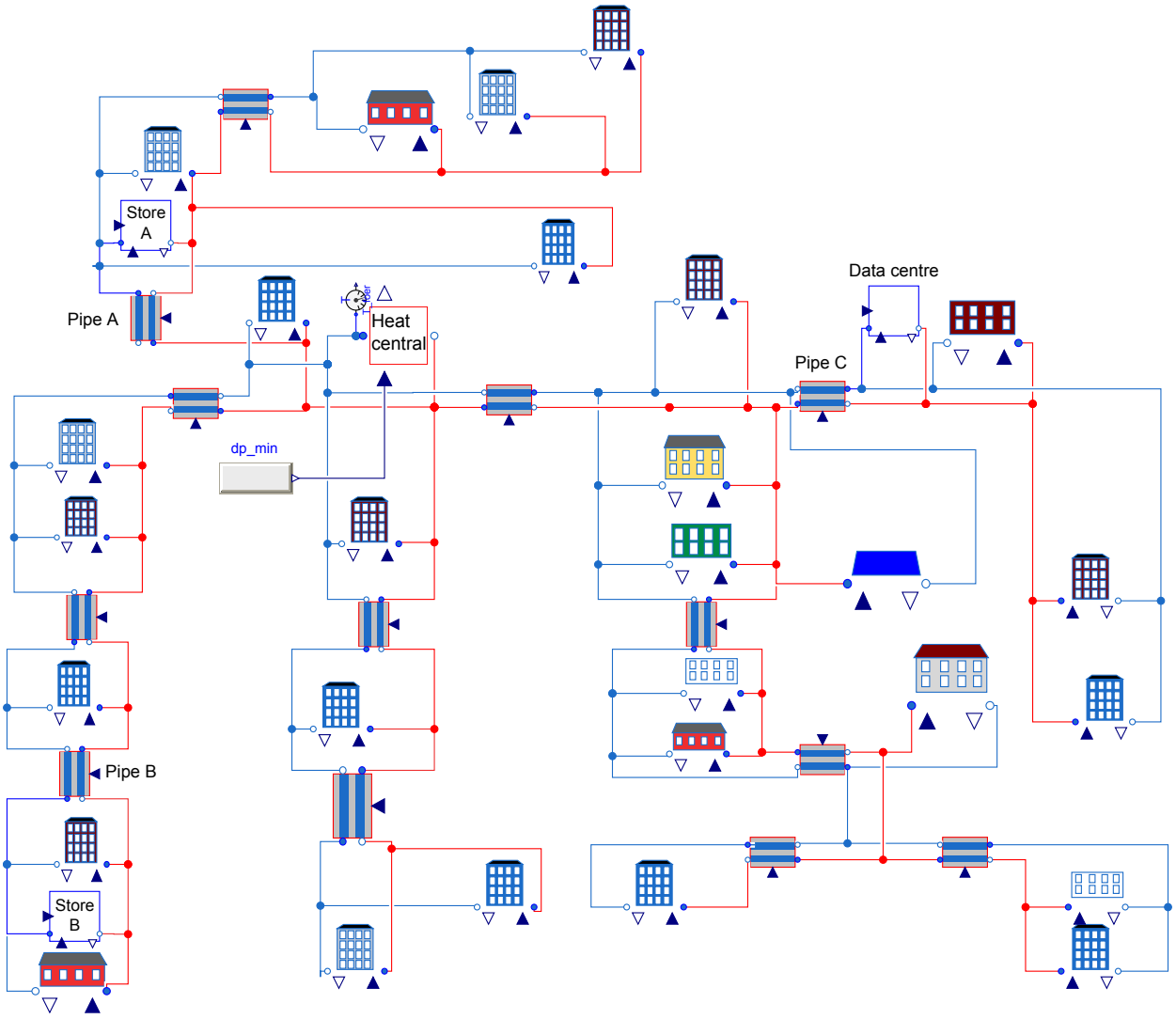

Figure 1: The modeled building area in Dymola, including different building types, piping, prosumers (a data center and two food retail stores) and a heat supply plant. The supply lines are denoted with red, and the return lines with blue.

where C_p is the specific heat capacity of water and $\dot{m}_{hot}$ and $\dot{m}_{cold}$ are the mass flows on the hot and cold side of the heat exchanger, respectively. The effectiveness is a complex function of the number of transfer units (NTU) and the heat capacity rates on the hot and cold side [21]:

$$\epsilon = f\left(NTU, \frac{C_{min}}{C_{max}}\right), \tag{3}$$

where C_{min}/C_{max} is equal to C_{cold}/C_{hot} or C_{hot}/C_{cold}, depending on the relative magnitudes of the hot and cold fluid heat capacity rates. NTU is a dimensionless parameter, defined as

$$NTU = \frac{UA}{C_{min}}, \tag{4}$$

where U is the average heat transfer coefficient and A the heat transfer area. Using the NTU approach, the simulation times were reduced by approximately 60 % (from 8 to 3 hours for the entire network) compared to the approach used in the previous study [7]. No heat losses were included in the heat exchanger model.

This is the accepted version of an article published in Energy.
DOI: 10.1016/j.energy.2018.03.033

2.2.2. Twin pipe model

In the previous model [7], separate pipes without thermal interaction were used for the supply and return lines. For the present model, a twin pipe model was developed. In a twin pipe, the supply and return lines were enclosed in the same insulated pipe and hence thermally coupled with each other in addition to the ground. To model this effect without extensive computational efforts, the correlations developed by [22] were used. In this approach, the heat loss from each pipe is split into two: (i) heat loss from the entire pipe to the ground (symmetrical problem), q_s, based on the average temperature in the pipes [22]:

$$q_s = (T_s - T_0)2\pi\lambda_i h_s \tag{5}$$

and (ii) heat loss from the hot to the colder pipe (asymmetric problem), q_a, based on the temperature difference between the two pipes:

$$q_a = T_a \cdot 2\pi\lambda_i \cdot h_a. \tag{6}$$

T_s is the average temperature between the two pipes, $T_s = \frac{T_1+T_2}{2}$, related to the symmetrical problem (i); T_a is the temperature difference between the two pipes divided by two, $T_a = \frac{T_1-T_2}{2}$, related to the asymmetric problem (ii); and T_0 is the temperature on the ground surface. T_0 was therefore assumed to be equal to the ambient temperature, based on [23]. λ_i is the thermal conductivity of the insulation, and h_s and h_a are the heat transfer coefficients for the symmetric and asymmetric problem, respectively. The heat loss from the supply (1) and and return (2) pipes is calculated by superposition:

$$q_1 = q_s + q_a \tag{7}$$

$$q_2 = q_s - q_a. \tag{8}$$

The heat transfer coefficients h_s and h_a are complex functions of the pipe geometry, and the thermal conductivities of the ground and of the pipe. The parameter values applied in the simulations are given in Table 1. For the pipe insulation, insulation series 2 was assumed. The thermal conductivity of the ground varies between 0.5 and 2.5 W/(mK) depending on soil type and moisture [23]. In Trondheim there are different types of soils, with a large share of wet clay, corresponding to the highest thermal conductivity. A value of 1.8 W/(mK), somewhat above the average of the two extrema, was chosen for the present study.

Table 1: Parameter values applied in the simulations.

Parameter name	Symbol	Value	Comment
Ground thermal conductivity	λ_g	1.8 W/(mK)	Based on [23]
Insulation thermal conductivity	λ_i	0.024 W/(mK)	From [24]
DHW temperature set-point HT/LT	-	65/60 °C	-
Radiator temperature set-point (winter/summer)	-	60/40 °C	Outdoor compensated
DH supply temperature HT (winter/summer)	T_{supply}	115/75 °C	Outdoor compensated
DH supply temperature LT	T_{supply}	65 °C	Constant
DH return temperature HT (winter/summer)	T_{return}	65/55 °C	Outdoor compensated
DH return temperature LT (winter/summer)	T_{return}	65/40 °C	Outdoor compensated

The pipe diameters were selected assuming a maximum pressure drop of 150 Pa/m, as this is a normal design criteria used by the local DH suppliers. Based on the Darcy-Weissbach equation and Colebrook's expression for friction factor [25][h. 522], a relationship between maximum mass flow $\dot{m}_{max}$ and inner diameter D_i was derived in [7]:

$$D_i = 0.0379 \cdot \dot{m}_{max}^{0.37}. \tag{9}$$

Hence, for a given maximum mass flow in a pipe, the equation gives the pipe diameter at a pressure drop of 150 Pa/m. The calculated diameter was always rounded up to the nearest real diameter available from DH pipe suppliers [24].

This is the accepted version of an article published in Energy.
DOI: 10.1016/j.energy.2018.03.033

2.2.3. *Customer substation*

For the building models, representing the customer substations, indirect connection with separate heat exchangers for domestic hot water (DHW) heating and space heating (SH) was applied. A schematic diagram of the model is shown in Fig 2. Mass flow in the DHW/SH (secondary) loops was controlled by the DHW/SH demands, based on real DH use data as explained in section 2.1. Different input data was applied for different types of buildings (see [7] for more details). Mass flow on the primary side was controlled with valves, based on set-points for supply temperature on the secondary side. For DHW heating, the desired supply temperature was 65 °C for the high-temperature (HT) simulations, and 60 °C for the low-temperature (LT) simulations. A temperature level of 8 °C was assumed for the incoming cold water. For SH, the supply temperature set-point for the radiators was outdoor compensated, with limits of 40/60 °C. The highest supply temperature was used from -20 °C and below, the lowest from 20 °C and above and a linear relationship between the two otherwise. Same limits were applied for HT and LT simulations.

As the heat demand was based on input data, heat loss from the buildings to the ambient was not included in the model. The radiator was set to exchange heat with a constant room temperature of 21 °C, and the mass flow in the SH loop was controlled by a pump to supply the required amount of heat, based on the SH demand. The radiator area was chosen based on the heated area of the building, and the maximum desired temperature difference in the radiator loop. The targeted return temperature was in the range 30-40 °C. The UA-value depended on the current radiator mass flow.

The UA-values for the DHW and SH heat exchangers were assumed constant and calculated separately for each building type. The values were based on the building's peak heating demand, and the logarithmic mean temperature difference for winter operation, based on the temperature limits given in Table 1. Two sets of UA-values were required for each building type; one for HT and one for LT simulations, as the supply- and return temperature limits were different for the two cases. On average, the UA-values for LT simulations were approximately 7.6 times larger than the UA-values for HT simulations for SH heat exchangers and 3.3 times larger for DHW heat exchangers.

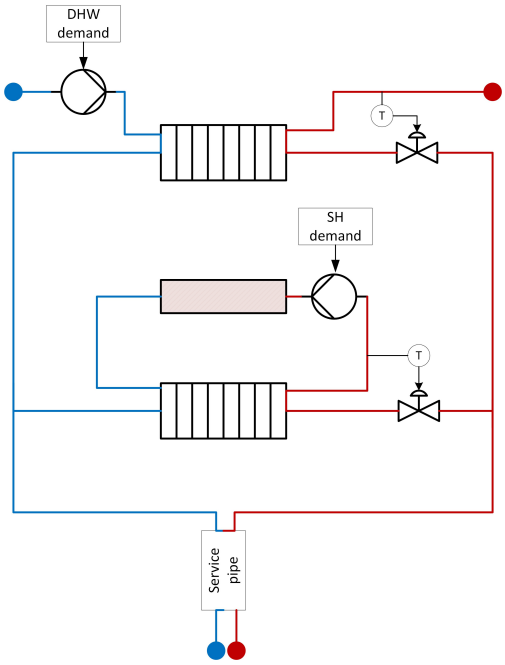

Figure 2: Schematic diagram for the customer substation model.

Every building connected to a DH grid has its own service pipe leading to only that building, as shown in Figure 2. Therefore, all building models also included a twin pipe before and after the heat supply system. The length of the service pipe was estimated based on the building plan (see [7]).

As the interest in the present study lies in the potential of prosumers and low-temperature heat distribution from

This is the accepted version of an article published in Energy.
DOI: 10.1016/j.energy.2018.03.033

the perspective of the DH provider, the building heat distribution system was not a part of the model. However, the modelled building area is a new area to be built in Trondheim (see section 2.1), and the latest building standards will apply. It was thereby presumed that the buildings will have a heat distribution system that is suited for lower distribution temperatures, such as floor heating.

2.2.4. Heat central

The heat central ensures that the required supply temperature level and pressure lift is provided for the system at each moment. In an actual grid this central could represent the interface to the primary DH grid. The required pressure lift is determined by the building furthest away from the central, for which the transportation of water to the building has highest pressure drop. In addition, every customer substation has pressure loss across its heat exchangers, and the local DH supplier in Trondheim guarantees a differential pressure of 70 kPa at the customers. Thus the heat supply plant model receives the pressure drop from the buildings furthest away as an input and applies a PI-controlled pump to keep the pressure drop at a minimum of 70 kPa for these customers. For buildings closer to the heat supply plant, the pressure drop is naturally higher than 70 kPa. This excess pressure head is throttled by the valves in the substation, and is hence pure hydraulic loss. No maximum capacity limit was assumed for the heat central; it simply delivers the heat that is required by the local DH grid. Finding the required capacity was thus a part of the results rather than an input.

For the circulation pump, a constant efficiency of 50 % was assumed, corresponding to the average efficiency of new commercial pumps. In reality, the pump efficiency is a function of the volume flow rate and pressure lift. Simulations with a pump with varying efficiency were tested in a previous study [7], however this gave no significant difference in total pump energy and resulted in lower simulation speed.

2.2.5. Heat prosumers

For the present study, two types of heat prosumers were included, likely to be present in urban neighborhoods: data centers and food retail stores. For both of these, the surplus heat source is a cooling/refrigeration system, and the availability of surplus heat depends on the ambient temperature, while at low ambient temperatures there might be a demand for heat. The surplus heat capacity of the prosumers was hence defined as follows:

$$\dot{Q}_{pros} = \dot{Q}_{pros,0} \cdot (1 + k) \cdot \frac{T_{amb} - T_{inv}}{25 - T_{inv}}, \tag{10}$$

where T_{amb} is the ambient temperature (in °C); T_{inv} is a parameter, equal to the ambient temperature level below which the supplier has a demand for heat; $\dot{Q}_{pros,0}$ is the baseline capacity for the surplus heat, available at $T_{amb} = T_{inv}$; and k is a gain factor for summer operation. 25 °C was the highest measured outdoor temperature, hence the capacity at this temperature level is equal to $\dot{Q}_{pros,0} \cdot (1 + k)$. The surplus heat capacity will become negative, i.e. there will be a heat demand, at $T_{amb} < T_{inv}$.

In practice having the ability to supply and receive heat in the same model was accomplished by having two separate loops, each with its own heat exchanger (see Figure 3): one for supplying heat, equipped with a pump to control the mass flow, and one for receiving heat, equipped with a valve. These loops are never active simultaneously, i.e., the mass flow is zero in the loop that is not active. During periods of heat supply, i.e., when $T_{inv} < T_{amb}$, the water to be heated is taken from the return pipe and delivered in the supply pipe, as illustrated in Figure 3. This type of connection, so-called R/S connection, has become the most common alternative for DH prosumers in Sweden, and has the largest potential according to [12]. During periods of heat demand, the flow is reversed; that is, water is taken from the supply pipe and delivered in the return pipe, as in a normal customer substation. Based on the availability of the surplus heat, the mass flow in the pump was controlled such that the temperature supplied to the grid would be 65 °C. This heat delivery temperature corresponds to the temperature the Pionen data center delivers to the DH hetwork in Stockholm [26]. Requiring a high enough supply temperature also enables to avoid the potential problems related to differential pressure [13]. Possible energy required for upgrading the heat was not considered in the model.

The values for T_{inv}, $\dot{Q}_{pros,0}$ and k applied in the simulations are given in Table 2. For the data center, lower values for T_{inv} and k were set with respect to the food retail store as it was assumed that data centers have surplus heat available all year round, and they are less affected by infiltration due to e.g. door openings, hence less dependent on the ambient temperature. In reality, free cooling is often applied in data centers in the wintertime, resulting in little surplus heat during these periods.

This is the accepted version of an article published in Energy.
DOI: 10.1016/j.energy.2018.03.033

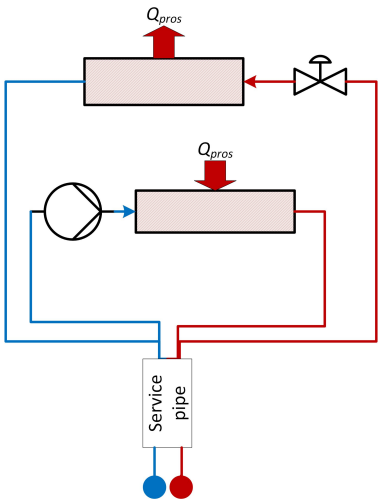

Figure 3: Schematic diagram for the prosumer model.

Two scenarios with different surplus heat capacities for the food retail stores and the data center were simulated, shown in Table 2. The heat capacities for the food retail store were chosen based on measurements from an existing store with surplus heat utilization [27]. The heat capacities for the data center were chosen keeping in mind the Pionen data center in Stockholm, which has a heat delivery of 600 kW during normal operation, with floor area of 1100 m^2 [26]. For the present case, somewhat smaller capacities (200 and 400 kW) were chosen, as the simulated building area was rather small and having such a large data center would not have been realistic. Annual surplus heat profiles for the data center and the food retail store at the lower capacity level are shown in Figure 4.

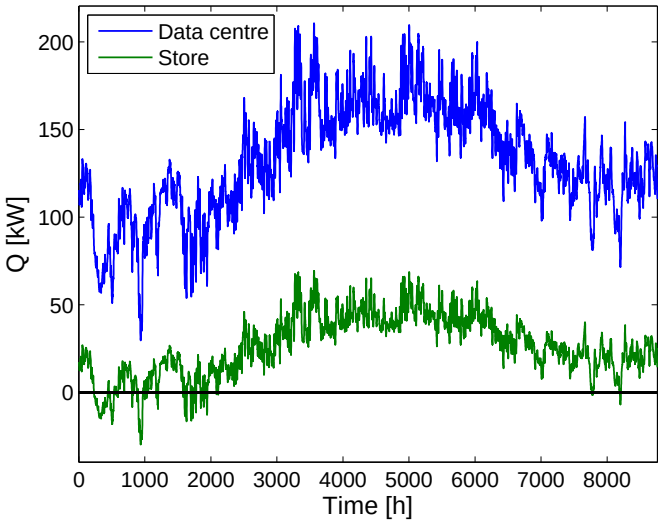

Figure 4: Annual surplus heat profiles for the data center and the food retail store.

The network included two retail stores and one data center. To study the effect of heat delivery on different parts of the network, one of the retail stores (store A) was placed nearby the heat central, while the other one (store B) was placed next to the customer lying furthest away from the heat central (see Figure 1).

In periods of high availability of surplus heat, the heat delivery and hence the mass flow from the prosumers might become so high that it exceeds the heat demand, and hence the mass flow available for supplying surplus heat in the

This is the accepted version of an article published in Energy.
DOI: 10.1016/j.energy.2018.03.033

grid. This problem called for a priority setting for when to receive heat from which prosumer, and the data center was given the first priority. In reality, the heat supplier with the first priority would be the one offering the lowest price. Pricing of surplus heat was not a part of the study, however the assumed priority setting in the model was equivalent to assuming a price ranking.

To apply the priority setting in practice, and to ensure that the heat supply from the prosumers never exceeded the demand, each prosumer was given a maximum allowed mass flow based on the mass flow available in the grid at each moment of time. The mass flow available is a function of the momentary heat demand and temperature lift in the heat central. The prosumer with the highest priority had access to maximum 95 % of the mass flow in the grid, the one with second highest priority had access to 95 % of the remaining mass flow and so on. The factor of 95 % was included as an additional safety margin to avoid exceeding the demand. If a surplus heat supplier did not have enough water available to do away with all its heat, the remaining heat was rejected to ambient.

2.3. Simulations

Four different scenarios were simulated:

- High-temperature (HT): Supply temperature outdoor compensated. The highest temperature level (115 °C) is used from -20 °C and below, the lowest (75 °C) from 15 °C and above, and a linear relationship is applied between the two otherwise. The heat demand is covered by the heat central. This scenario represents the current practice for the main DH network in Trondheim.
- Low-temperature (LT): Constant supply temperature of 65 °C. The heat demand is covered by the heat central.
- Low-temperature with prosumers 1 (LTP1): Constant supply temperature of 65 °C. The heat demand is covered by the heat central and three distributed prosumers (one data center and two food retail stores) at a lower capacity level (see section 2.2.5 and Table 2).
- Low-temperature with prosumers 2 (LTP2): As LTP1, but with a higher capacity level for the three prosumers.

The return temperature limits for the HT and LT simulations were given in Table 1. In the previous study [7], different supply temperature levels were considered, however for the present study 65 °C was chosen as this represents the potential future temperature level, considering the Norwegian legislation.

Table 2: Parameter values applied for the surplus heat providers in the two scenarios including prosumers, LTP1 and LTP2.

		$\dot{Q}_{pros,0}$ [kW]	T_{inv} [°C]	k
LTP1	Data center	200	-25	0.05
	Food retail store	60	-5	0.15
LTP2	Data center	400	-25	0.05
	Food retail store	100	-5	0.15

2.4. Calculation of the CO_2 equivalent emissions

The GHG emissions for heating were calculated from the basis of the total annual simulated heat flow in the heat central. The DH supplier in Trondheim applies many different heat sources, and the same sources were assumed to be available for the heat central in the present study. The GHG emissions for the different sources were found from [28] and [29]. It was assumed that each energy source has a fixed maximum capacity, and that the least polluting sources would be used first. The only exception is waste incineration, which the supplier is decreed to perform, and must thus always have the first priority. As the HT scenario represents the current operation strategy, it was assumed that the given energy mix – i.e., the relative share of the heat sources applied by the DH supplier – is valid for this scenario. Capacity limits for each energy source were thus calculated based on the HT scenario. The same capacity limits were applied for the other simulated scenarios. The energy required for the circulation pumps was also included in the calculations. For calculating the emissions for electricity, Nordic electricity mix was assumed [28]. For surplus heat delivery, zero emissions were assumed, as any energy needed for upgrading the heat was not considered.

This is the accepted version of an article published in Energy.
DOI: 10.1016/j.energy.2018.03.033

3. Results

3.1. Overall comparison

Table 3 summarizes the results for total annual delivered heat by the heat central and the prosumers, as well as the total annual heat losses and pump work for the four simulated scenarios. For the LT scenario, the reduction in heat delivered by the heat central is only 1 % with respect to the reference (HT) scenario, and this is solely due to the reduction in heat losses. For the LTP1 and LTP2 scenarios with surplus heat delivery, the reduction is 13 and 25 %, respectively. The heat losses are reduced by 20 % for the LT scenario, and by 22 % for the LTP scenarios. The fact that the heat losses are lower for the LTP scenarios than for the LT scenario despite the same supply temperature is due to the distributed heat supply, yielding lower heat transportation distances.

The total pump work is increased by 61 % for the LT scenario and 68 % for the LTP scenarios; however, the pump work is an order of magnitude lower than the heat losses. The work delivered by the pumps at the surplus heat suppliers is included in the total pump work.

Table 3: Results for total annual heat delivered by the heat central (Q_{hc}) and the prosumers (Q_{pros}), as well as the total annual heat losses and pump work. In addition, total heat losses and pump work relative to the total delivered heat (Q_{del}) are given. Q_{del} includes heat from both the heat central and the prosumers. The pump work includes the work done by the pumps at the prosumers.

Case	Q_{hc} [GWh]/(%)	Q_{pros} [GWh]	Q_{loss} [MWh]/(%)	W_{pump} [MWh]/(%)	$\frac{Q_{loss}}{Q_{del}}$ (%)	$\frac{W_{pump}}{Q_{del}}$ (%)
HT	13.4 / 100	0	609 / 100	13 / 100	4.56	0.10
LT	13.3 / 99	0	489 / 80	21 / 161	3.68	0.16
LTP1	11.7 / 87	1.63	477 / 78	22 / 168	3.59	0.16
LTP2	10.0 / 75	3.26	477 / 78	22 / 168	3.59	0.16

The relative heat losses are in general low; between 3.6 and 4.6 %. The heat loss per meter grid (trench) was 10.2 W/m for the HT scenario, 8.2 W/m for the LT scenario and 8.0 W/m for the LTP scenarios. These are very similar to the values given by the pipe producer (7.2-8.7 W/m) [30]. The fact that the relative heat losses are low is thus due to the well-insulated twin pipes. Furthermore, the heat losses here includes only the losses in the pipelines; potential losses at the heat central or customer substations have not been taken into account.

Figure 5 shows the duration curves for the delivered heat for the different scenarios, with an insert showing the first 150 hours. As can ben seen from the figure, the difference in peak demand between the four scenarios is minimal, as the surplus heat supply is significant in the summertime, but low during the coldest periods.

In a previous study [7], the same building area was modelled at supply temperatures of 55, 65 and 95 °C, with more simplified models for e.g. pipes (single pipes), valves (controlling flow area rather than mass flow), and customer substations. The net demand in the present study is 1.4 GWh higher than in [7], which can be attributed to the different input data for apartment blocks (see section 2.1). The heat loss per meter grid line (trench) was 15.9 W/m for the previous simulation at 65 °C supply temperature, which is clearly higher than for the present LT scenario (8.2 W/m). This reduction in heat losses is obviously due to the application of twin pipes.

Figure 6 shows additionally the mass flow rate delivered by the heat central as a function of ambient temperature for the different scenarios. The mass flow rate is clearly higher for all the LT scenarios as compared to the HT scenario at ambient temperatures below 0-5 °C. At ambient tempeartures above 10 °C, the mass flow is on average lower for the LT scenarios. This effect is pronounced for the LTP2 scenario owing to the fact that during summertime a large share of heat demand is covered by the prosumers.

In the summertime, the heat demand is dominated by the DHW demand. The fact that the mass flow rate is lower in the summertime for the LT scenarios with respect to the HT scenarios, is hence related to the size of the DHW heat exchangers and temperature difference in the heat exchangers. For HT, the temperature difference at the heat exchanger inlet on the primary side is in the summer time 10 °C. For LT scenarios, this temperature difference is 5 °C, but the heat exchanger area is 3.3 times higher (see section 2.2.3); thereby a lower mass flow is required to obtain the same heat flow rate.

3.2. Surplus heat delivery

Figure 7 presents the share of the total heat demand covered by the prosumers and the heat central for the two scenarios including prosumers, LTP1 and LTP2. For the LTP1 scenario, the surplus heat delivery by the prosumers is

This is the accepted version of an article published in Energy.
DOI: 10.1016/j.energy.2018.03.033

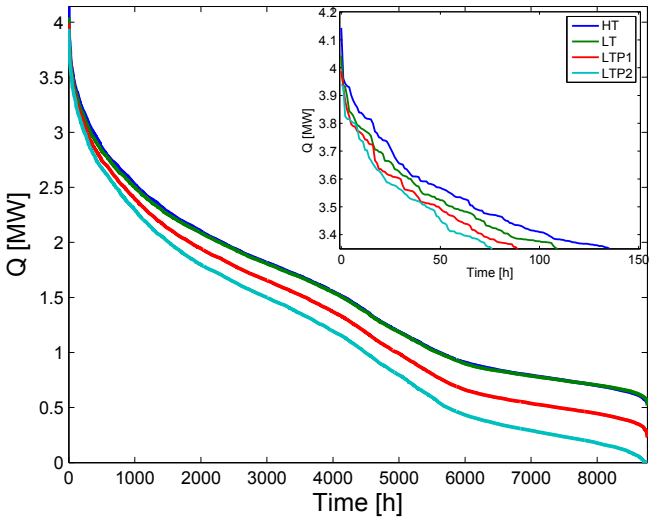

Figure 5: Duration curves for heat delivered by the heat central for the different simulated scenarios. The insert displays the duration curves for the first 150 hours, showing the difference in the peak demand.

between 40-50 % during the summertime, and between 5 and 20 % in the spring and autumn. For the LTP2 scenario, the contribution from the prosumers is up to 80-90 % during summer, and considerable (10-30 %) also during spring and autumn.

To investigate the effect of the surplus heat supply on the pipe mass flow, the mass flow in the twin pipes residing closest to the prosumers, marked as Pipe A, B and C in Figure 1, is plotted in Figure 8 (a) and (b) for LTP1 and LTP2, respectively. In the summertime, the flow becomes negative for pipe C beside data center and to a larger degree also for pipe B beside store B, in particular in the LTP2 scenario. This indicates that the prosumer is in this period able to cover the heat demand for this part of the grid, and shows also that the model is able to handle bidirectional flow. For pipe B, the mass flow is approximately zero for most of the summer in the LTP1 scenario, which indicates that store B is able to cover the heating demand for the two buildings for this period. In the LTP2 scenario, with higher capacities, the data center is providing heat for the buildings beyond pipe C frequently also during winter, and in particular during autumn.

The fact that the flow in pipe A close to store A is positive all the time is because this store is located far away from the end of the branch. That is, beyond store A there are more buildings to supply heat for than in the case of store B, and additional heat delivery from the heat central is required to be able to cover the heat demand for these buildings.

Figure 9 (a) shows additionally the heat delivered by the heat central and by the prosumers for a particular day in March with high surplus heat supply. Figure 9 (b) shows the mass flow in pipes A, B and C for the same period. Figure 9 (a) demonstrates that the heat delivery by the prosumers peaks around noon when T_{amb} is the highest, while the heat demand in the grid, reflected in the heat delivered by the heat central, peaks in the morning. From Figure 9 (b) it can be seen that the mass flow profile in pipe A reflects very precisely the heat delivery by the heat central, while the mass flow profiles for pipes B and C are more affected by the heat supply from the prosumers, as could be expected.

3.3. CO_2 emissions

The reduction in CO_2 emissions is considered from two perspectives: (i) considering the heat delivery by heat central alone, in order to analyze how the local heat production affects the energy mix from the DH provider; and (ii) looking at the total heat delivery in the local grid, including the surplus heat supply. Table 4 shows the total equivalent CO_2 emissions for these two perspectives for the different scenarios, as well as the reduction in emissions relative to the HT scenario. The calculations for (i) includes the emissions from the heat delivery and the pump work by the heat central, and for (ii) the surplus heat (emission-free) and the pump work at the prosumers in addition. These two figures

This is the accepted version of an article published in Energy.
DOI: 10.1016/j.energy.2018.03.033

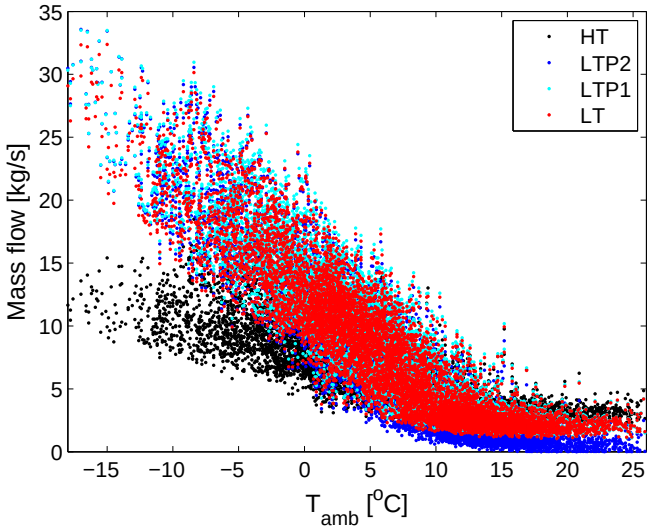

Figure 6: Mass flow delivered by the heat central as a function of ambient temperature for the different simulated scenarios

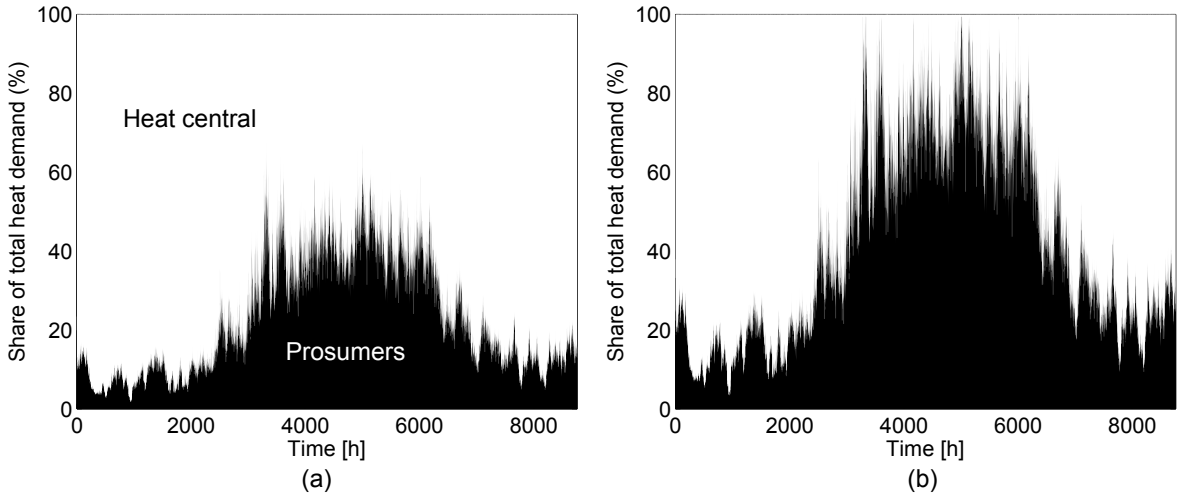

Figure 7: The share of heat delivered by the prosumers and by the heat central with respect to the total heat demand: (a) LTP1 and (b) LTP2.

are obviously equal for the HT and LT scenarios where no prosumers are included. Furthermore, the total emissions are almost equal for the HT and LT scenarios, as the difference in the amount of heat delivered by the heat central is only 1 % between these two scenarios. Hence the overall environmental impact of lowered distribution temperature alone is hardly noticeable, at least for a grid with low heat loss values as considered in this study.

For the scenarios including prosumers, a considerable reduction in the emissions is obtained, in particular when considering the surplus heat delivery (reduction of 16/29 % for the LTP1/LTP2 scenarios), but also when looking at the heat delivery by the heat central alone (5/6 % for LTP1/LTP2). This is an important result, showing that local heat supply can contribute to reduction in the use of more polluting peak heating sources at the DH provider. This can be mainly attributed to the lowered demand for heat from the heat central, but also to some extent the lowered heat losses for the LTP scenarios (see section 3.1 and Table 3). The emissions considering the total delivered heat are lower, because they include the heat from prosumers and are thereby divided by a larger amount of heat than the emissions for heat delivered by the heat central alone.

This is the accepted version of an article published in Energy.
DOI: 10.1016/j.energy.2018.03.033

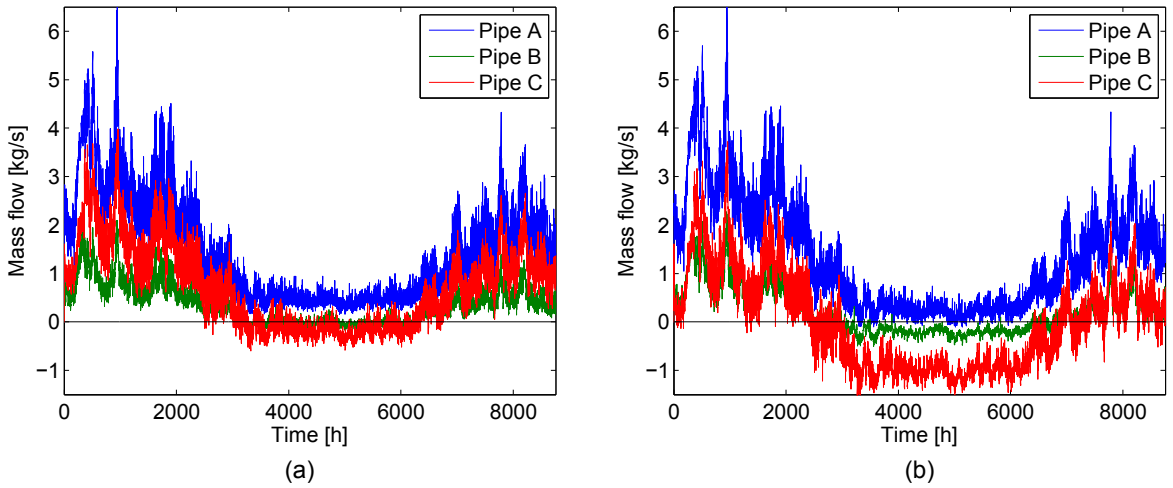

Figure 8: Mass flows in the pipes nearby surplus heat suppliers: (a) LTP1 and (b) LTP2. For the location of the pipes, see Figure 1.

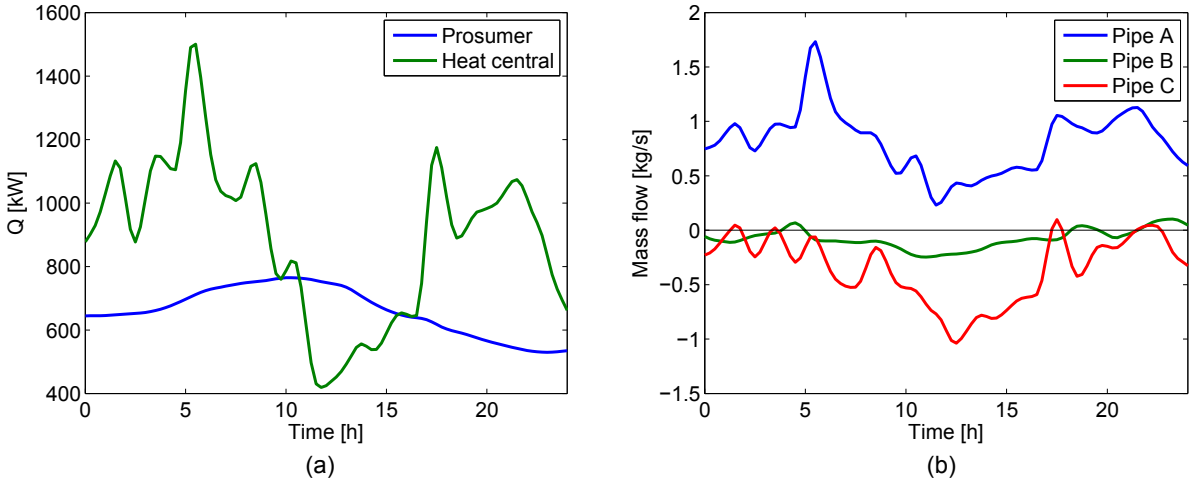

Figure 9: (a) The total heat delivery by the prosumers and the heat central for the LTP2 scenario, considering a 24-hour period in March and (b) the mass flow in pipes A, B and C for the same period.

Figure 10 shows the distribution of the applied heat sources used in the four simulated scenarios, looking at the total heat delivery in the local grid. The results were obtained as explained in section 2.4; by assuming the energy mix for the HT scenario to be equal to the energy mix at the local DH supplier, and further assuming the same capacities for the heat sources for each simulated scenario. The distribution is practically the same for the HT and LT scenarios as the difference in the amount of heat delivered by the heat central is so small for these two scenarios. The LTP scenarios are clearly different from the HT and LT scenarios. Looking at Figure 10, most obvious is the reduction in the total share of heat received from waste incineration: from 73 to 66/57 % for LTP1/LTP2. Less visible in the figure is the relative reduction in the use of more polluting heat sources from the perspective of the heat central: 21/24 % reduction for electricity, and 18/28 % for the remaining heat sources, including biogas and liquefied petroleum gas (LPG). Furthermore, from the perspective of the heat central, the relative amount of heat from waste incineration was increased by 2-3 %. It should be noted that the energy mix applied in the calculations is based on the DH system in Trondheim and the results are hence not directly transferable to other systems.

This is the accepted version of an article published in Energy.
DOI: 10.1016/j.energy.2018.03.033

Table 4: CO_2 equivalent emissions for the heat delivered by the heat central, and for the total heat delivery. The total heat delivery includes the surplus heat and the pump work at the prosumers. The total emissions per kWh produced heat is given, as well as the reduction in emissions relative to the HT scenario.

	Heat delivered by the heat central		Total delivered heat	
	[g/kWh]	Reduction in %	[g/kWh]	Reduction in %
HT	23.8	-	23.8	-
LT	23.6	1.1	23.6	1.1
LTP1	22.7	4.8	19.9	16.4
LTP2	22.4	5.9	17.0	28.9

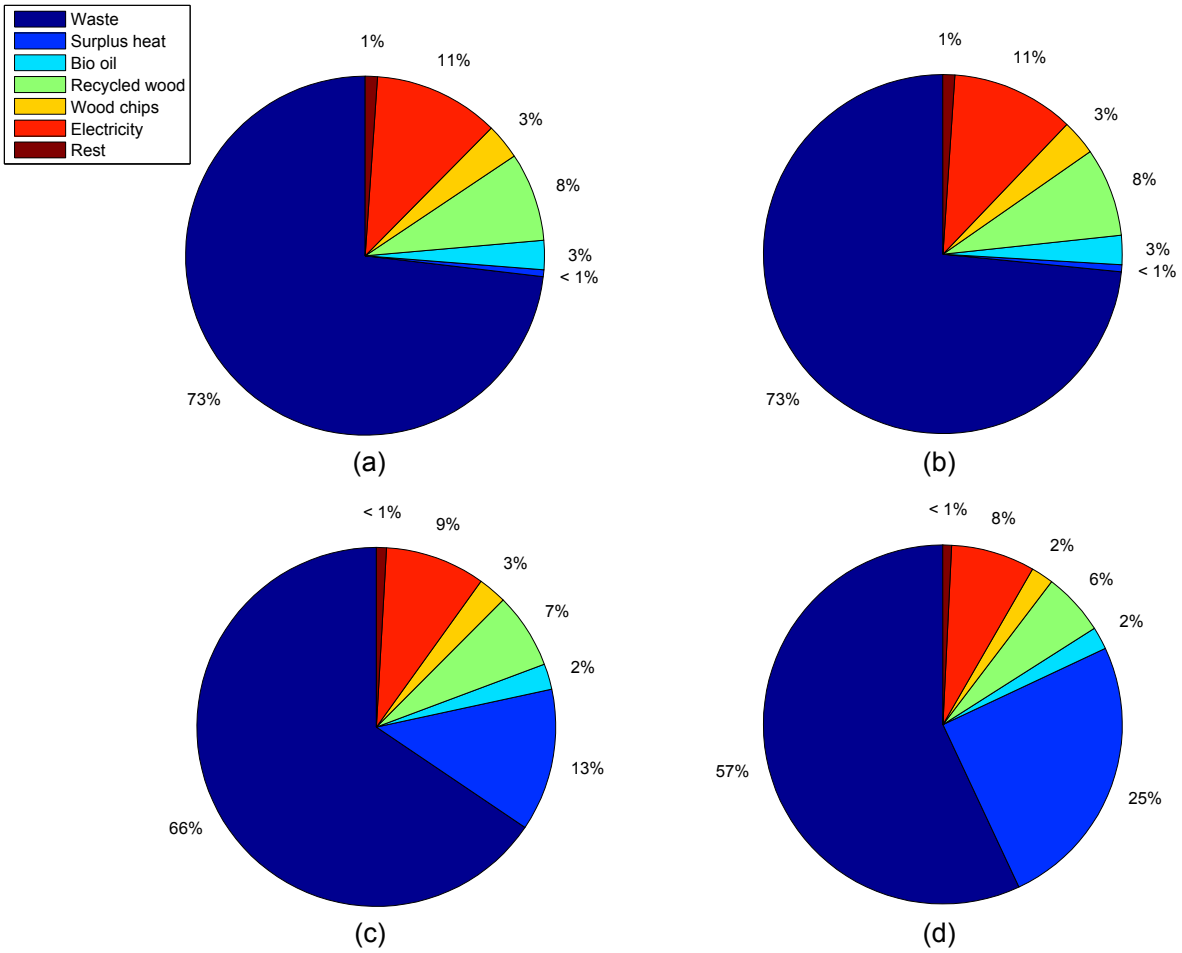

Figure 10: The share of heat received from different heat sources for the different simulated scenarios: (a) HT, (b) LT, (c) LTP1, (d) LTP2. The "rest" includes LPG and biogas.

4. Discussions and conclusions

There is a high potential for utilization of local low-temperature surplus heat in small-scale DH grids. In the present simulation case study, considering a building area with two retail stores and a data center as the surplus heat suppliers, a reduction of up to 25 % in the demand for delivered heat was obtained as compared to a high-temperature reference scenario. Regarding the environmental impact, a considerable reduction in CO_2 equivalent emissions was obtained when considering the total heat delivery, including the emission-free surplus heat supply. A clear reduction in the emissions was however obtained also when looking at the heat delivery by the heat central alone, showing that

This is the accepted version of an article published in Energy.
DOI: 10.1016/j.energy.2018.03.033

local heat supply can contribute to a reduction in the use of more polluting peak heating sources at the DH provider. The reduction in emissions can be mainly attributed to the lowered demand for delivered heat, but to some extent also to the lowered heat losses, resulting from overall lower heat transport distances in a DH grid including local, decentralized heat suppliers.

A problem with the type of prosumers considered in the present study, with surplus heat source being a refrigeration or cooling system, is that the availability of surplus heat is highest during the summer. The reduction in the annual peak heating demand is hence minimal. Seasonal thermal energy storage may be needed for extended utilization of the surplus heat, as suggested by [8]. Moreover, the heat supply from the prosumers peaks around noon, while the overall heat demand is the highest in the morning. Diurnal thermal storage could be applied to reduce the peak heating load in the heat central in the mornings, and hence to further reduce the environmental impact of the DH system. Diurnal thermal storage systems in the form of e.g. water tanks are generally easier to implement than seasonal thermal storage systems, and should be included in a further study.

In periods, the heat production by the prosumers may be sufficient to cover the entire heating demand for the grid segment it is located in. This induces flow reversals in the pipeline, which was handled well by the model. This was also demonstrated in a previous dynamic modeling study by Schweiger et al. [18]. The results from the present study hence further confirm that dynamic modeling suits well for simulating and analyzing small-scale DH grids with decentralized heat supply.

Another challenge associated with prosumers is that the differential pressure at the customers might drop, as suggested in [12, 13]. This problem was not observed in the present study, probably owing to the fact that the prosumers were assumed to deliver heat at a constant, high (65 °C) temperature. In the previous studies by Brand and Lennermo et al [12, 13], heat supply from solar collectors with varying, lower supply temperature was considered, yielding locally higher flow velocities and hence lower pressures. Nevertheless, in a grid with distributed heat suppliers, the location of the customer with lowest differential pressure will alter, depending on the location of the prosumers and their surplus heat delivery. In the present study, the required pressure lift at the heat central was determined by the building furthest away, however a more advanced control strategy would be needed in a grid including prosumers. This should be taken into account in a further study.

Losses not included in the present calculations are the heat losses in the heat exchangers, and the losses related to the production of heat. The latter is out of the scope of the present study, and the losses in the heat exchangers are considered to be minimal compared to the heat losses in the pipes.

Moreover, not considered in this study are the economic aspects related to low-temperature DH and utilization of local surplus heat. In many cases, surplus heat utilization may be beneficial from energetic and environmental point of view, but not profitable for the DH supplier. With the present supply temperature levels, upgrading the surplus heat is often necessary, which reduces the cost-efficiency. Introduction of 4th generation, low-temperature DH systems is hence crucial to increase the profitability of surplus heat delivery. It is also uncertain, which party should be responsible for the investment and operation costs of the required infrastructure, possibly including a heat pump for upgrading the heat. Furthermore, cost schemes for the surplus heat delivery are required, currently not existing in Norway. Finally, increase in investment costs due to e.g. larger heat exchangers needed at lower distribution temperatures should be taken into account.

To summarize; a possible future study should include diurnal thermal storage systems for extended utilization of surplus heat, take into account the energy required for upgrading the heat, and incorporate a more advanced control strategy to define the required pressure lift in a grid including prosumers. In addition, the economic aspects related to surplus heat delivery and reduction in the distribution temperature should be considered.

Acknowledgements

The authors greatly acknowledge support from the Research Council of Norway (RCN) under projects Development of Smart Thermal Grids (grant agreement (GA) number 245355), INTERACT (GA number 228656) and FME HighEFF (GA number 257632).

This is the accepted version of an article published in Energy.
DOI: 10.1016/j.energy.2018.03.033

References

[1] T. Laajalehto, M. Kuosa, T. Mäkilä, M. Lampinen, R. Lahdelma, Energy efficiency improvements utilising mass flow control and a ring topology in a district heating network, Applied thermal engineering 69 (1) (2014) 86–95.

[2] D. Connolly, H. Lund, B. V. Mathiesen, S. Werner, B. Möller, U. Persson, T. Boermans, D. Trier, P. A. Østergaard, S. Nielsen, Heat Roadmap Europe: Combining district heating with heat savings to decarbonise the EU energy system, Energy Policy 65 (2014) 475–489.

[3] H. Lund, S. Werner, R. Wiltshire, S. Svendsen, J. E. Thorsen, F. Hvelplund, B. V. Mathiesen, 4th Generation District Heating (4GDH): Integrating smart thermal grids into future sustainable energy systems, Energy 68 (2014) 1–11.

[4] D. Schmidt, A. Kallert, M. Blesl, S. Svendsen, H. Li, N. Nord, K. Sipilä, Low temperature district heating for future energy systems, Energy Procedia 116 (2017) 26–38.

[5] A. Dalla Rosa, J. E. Christensen, Low-energy district heating in energy-efficient building areas, Energy 36 (12) (2011) 6890–6899.

[6] M. Köfinger, D. Basciotti, R. Schmidt, E. Meissner, C. Doczekal, A. Giovannini, Low temperature district heating in Austria: Energetic, ecologic and economic comparison of four case studies, Energy 110 (2016) 95–104.

[7] H. Kauko, K. H. Kvalsvik, D. Rohde, A. Hafner, N. Nord, Dynamic modelling of local low-temperature heating grids: a case study for Norway, Energy 139 (2017) 289–297.

[8] L. Brange, J. Englund, P. Lauenburg, Prosumers in district heating networks - a Swedish case study, Applied Energy 164 (2016) 492–500.

[9] T. Ommen, W. B. Markussen, B. Elmegaard, Lowering district heating temperatures - Impact to system performance in current and future Danish energy scenarios, Energy 94 (2016) 273–291.

[10] U. Persson, B. Möller, S. Werner, Heat Roadmap Europe: Identifying strategic heat synergy regions, Energy Policy 74 (2014) 663–681.

[11] Fortum Värme, Open district heating, https://www.opendistrictheating.com, accessed: 2017-10-12 (2017).

[12] G. Lennermo, P. Lauenburg, L. Brand, Decentralised heat supply in district heating systems: Implications of varying differential pressure, in: The 14th International Symposium on DH and Cooling, September 7th to September 9th, 2014, Stockholm, Sweden, 2014.

[13] L. Brand, A. Calvén, J. Englund, H. Landersjö, P. Lauenburg, Smart district heating networks - A simulation study of prosumers impact on technical parameters in distribution networks, Applied Energy 129 (2014) 39–48.

[14] L. Giraud, R. Baviére, M. Vallée, C. Paulus, Presentation, validation and application of the districtheating modelica library, in: Proceedings of the 11th International Modelica Conference, Linköping University Electronic Press, 2015.

[15] D. Olsthoorn, F. Haghighat, P. A. Mirzaei, Integration of storage and renewable energy into district heating systems: A review of modelling and optimization, Solar Energy 136 (2016) 49–64.

[16] D. Basciotti, R. Schmidt, Peak reduction in district heating networks: a comparison study and practical considerations, in: The 14th International Symposium on District Heating and Cooling, 2014.

[17] F. Soons, J. I. Torrens, J. Hensen, R. D. Schrevel, A modelica based computational model for evaluating a renewable district heating system, in: 9th International Conference on System Simulation in Buildings, 2014.

[18] G. Schweiger, P.-O. Larsson, F. Magnusson, P. Lauenburg, S. Velut, District heating and cooling systems - Framework for Modelica-based simulation and dynamic optimization, Energy 137 (2017) 566–578.

[19] Modelon, Dymola, http://www.modelon.com/products/dymola, accessed: 2017-10-12 (2017).

[20] M. Wetter, M. Bonvini, T. S. Nouidui, Equation-based languages - A new paradigm for building energy modeling, simulation and optimization, Energy and Buildings 117 (2016) 290–300.

[21] F. P. Incropera, D. P. Dewitt, T. L. Bergman, A. S. Lavine, Principles of Heat and Mass transfer, Wiley, 2013, Ch. 11.

[22] P. Wallentén, Steady-state heat loss from insulated pipes, Licentiate Thesis, Report TVBH-3017, Dept. of Building Physics, Lund Institute of Technology, Sweden.

[23] A. Dalla Rosa, H. Li, S. Svendsen, Method for optimal design of pipes for low-energy district heating, with focus on heat losses, Energy 36 (5) (2011) 2407–2418.

[24] Logstor, https://www.logstor.com, accessed: 31.05.2017 (2017).

[25] F. P. Incropera, D. P. Dewitt, T. L. Bergman, A. S. Lavine, Principles of Heat and Mass transfer, Wiley, 2013.

[26] Fortum, Bahhof Pionen - Profitable recovery with Open District Heating, https://www.opendistrictheating.com/media/open-district-heating-bahnhof-pionen.pdf, accessed: 12.10.2017 (2016).

[27] S. Tønseth, Drastic cut in electricity bill for supermarket (June 2014).

[28] E. T. Otterlei, Klimaregnskap for fjernvarme, Tech. rep., Norsk Fjernvarme (2014).

[29] J. Gode, F. Martinsson, L. Hagberg, A. man, J. Hglund, D. Palm, Miljöfaktaboken 2011: Estimated emission factors for fuels, electricity, heat and transport in Sweden, Tech. rep., Värmeforsk (2011).

[30] Logstor, Dokumenterede lambdaværdier, https://www.logstor.com/media/1833/lambda-values_dk_p_dh.pdf, accessed: 2017-11-14 (2016).

This is the accepted version of an article published in Energy.
DOI: 10.1016/j.energy.2018.03.033